Association of the Anticancer Antibiotic Chromomycin A_3 with the Nucleosome: Role of Core Histone Tail Domains in the Binding Process

Mohd. Ayoub Mir and Dipak Dasgupta*

Biophysics Division, Saha Institute of Nuclear Physics, 37 Belgachhia Road, Kolkata-700 037, India

Received April 11, 2001; Revised Manuscript Received July 9, 2001

ABSTRACT: The anticancer antibiotic chromomycin A_3 is a transcription inhibitor which forms two types of complexes with Mg^{2+}: complex I (1:1 in terms of chromomycin A_3-Mg^{2+}) and complex II (2:1 in terms of chromomycin A_3-Mg^{2+}). These complexes are the DNA-binding ligands. With the broad objective of elucidation of the mechanism for action of this group of transcription inhibitors in eukaryotic systems, we have studied the interaction of the antibiotic with nucleosome core particles under different conditions. We have demonstrated and characterized the role of core histone proteins, particularly the N-terminal tail domains, in the association of nucleosome with both complexes of chromomycin. From a scrutiny of the spectroscopic features of the two bound complexes and comparison of the binding and associated thermodynamic parameters, we have shown the following. Core histone(s) stand(s) in the way of access of the ligand(s) to nucleosomal DNA. N-Terminal intact and chopped core particles interact differentially with the same complex. The modes of interaction of the two complexes, I and II, with the same system are different. Tryptic removal of N-terminal tail domains of core histones enhances the binding potential and access of both complexes of chromomycin to the nucleosomal DNA. Agarose gel electrophoresis of an equilibrium mixture containing either complex I or complex II and a saturating concentration of the core particle has demonstrated that both complexes have a tendency to disrupt the nucleosome structure, leading to a release of nucleosomal DNA. Compared to the N-terminal intact nucleosome, the N-terminal chopped nucleosome is more susceptible to disruption. Therefore, we suggest from the above results that the N-terminal tail domains, which have an important role in eukaryotic gene expression, stand in the way of a free access of external agents such as anticancer drugs to the eukaryotic genome. The significance of the results to understand the molecular basis of the transcription inhibitory capacity of chromomycin is discussed.

Chromomycin A_3 (abbreviated as CHR; structure shown in Figure 1), an antitumor antibiotic (*1*) of the aureolic acid group, is produced from *Streptomyces griseus*. It was clinically employed for testicular carcinoma and Paget's disease (*1*). At present its use is limited for its cytotoxic and immunosuppressive properties. Antitumor properties of the antibiotic in experimental tumors have been ascribed to its inhibitory role in the replication and transcription process during macromolecular biosynthesis (*1*, *2*). The prime cellular target of this antibiotic is DNA. A bivalent metal ion, such as Mg^{2+}, is an essential requirement at and above neutral pH for the (G/C) base-specific association via the minor groove with DNA (*3*).

Previous studies from our laboratory have shown that CHR forms two different types of complexes with Mg^{2+} in the absence of DNA. The stoichiometries of these complexes are 1:1 (complex I) and 2:1 (complex II) in terms of antibiotic$-Mg^{2+}$ (*4*−*6*). They are the potential DNA-binding ligands at and above physiological pH. They approach the target DNA via the minor groove (*4*−*6*). DNA-binding properties of this antibiotic have been very well studied in different laboratories including ours (*4*−*10*). In contrast, there have been very few studies on the association of this class of antibiotics with chromatin or nucleosome.

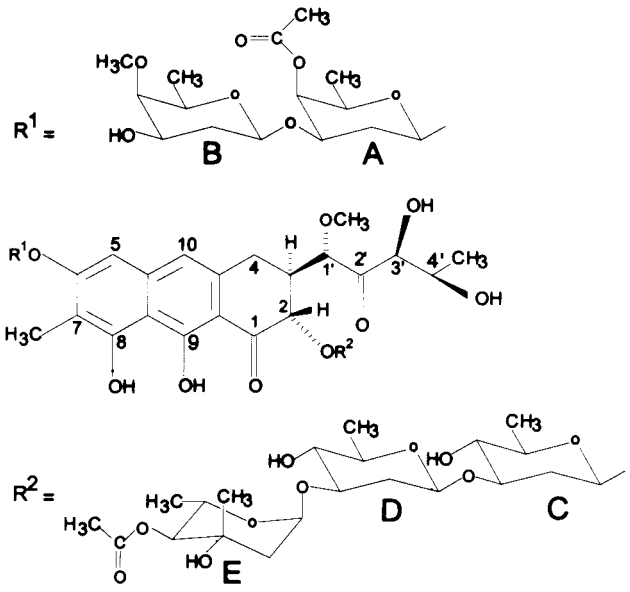

FIGURE 1: Structure of chromomycin A_3 (abbreviated as CHR in the text).

It is now well established that the packaging of DNA in the eukaryotic nucleus, the principal target site of the

* Corresponding author. Fax: +91 (33) 337 4637. E-mail: dipak@biop.saha.ernet.in.

10.1021/bi010731r CCC: $20.00
Published on Web 08/30/2001

antibiotic, involves several distinct hierarchical events. The first level of compaction occurs when DNA is wrapped around an octamer of core histones to form the repeating subunit nucleosome. An additional stretch of linker DNA connects the adjacent nucleosomes. The linker DNA and nucleosome core are associated with linker histone H1 (*11*). Each of the four core histones comprises a structured central domain, an amino-terminal tail, and in some cases a carboxy-terminal tail (H2A and H3) (*12*). The high-resolution structure of the nucleosome core particle (*13*) has shown that two turns of the DNA superhellix in the nucleosome core are arranged in such a way that they create sufficient gaps for the amino-terminal tails of both H2B and H3 histones to pass through to outside of the core particle. H2A and H4 tails pass across the superhelix on the flat faces of the particle to the outside as well. Histone tails are exposed. They are posttranslationally modified by acetylation and phosphorylation during eukaryotic transcription. Both modifications alter the charge distribution pattern on the N-terminal tails. It is an essential requirement for the eukaryotic gene expression (*14*). The tail domains also play an important role in the access of transcription factors and other DNA-binding proteins to the nucleosomal templates. Trypsinized nucleosomes leading to chopped N-terminal tails have been found to be more accessible to transcription factors such as TFIIIA (*15*), DNase cleavage, and other sequence-specific DNA-binding proteins (*16*, *18*, *19*). Thus the tails can impede access of proteins to nucleosomal DNA (*14*).

So far, there is only one report which shows the binding of CHR with chromatin isolated from mouse and rat liver (*20*). This preliminary study had the following lacunae. The concentration of CHR used was greater than 50 μM, and the Mg^{2+}concentration used was in micromolar range (45−328 μM). A mixed population of complexes I and II is formed under these conditions. Knowledge about the various levels of the chromatin structure was also not available then. Recently, we have reported the interaction of the related antibiotic mithramycin with rat and chicken liver chromatin (*10*).

This paper describes studies on the interaction of both complexes of CHR with N-terminal intact/chopped nucleosome core particle and DNA stripped of histone proteins from rat liver. The objectives of the study are as follows. First, we want to examine the effect of histones, in general, and their N-terminal tail domains, in particular, upon binding potential and energetics of association of the antibiotic−Mg^{2+} complexes with the nucleosomal DNA. Second, we want to examine the abilities of these complexes for nucleosome disruption and the role of N-terminal tail domains, if any, in this process. Finally, we have checked whether the earlier reported distinctive nature of the two complexes as linear DNA-binding ligands (*4*, *6*) still remains at the level of nucleosome where DNA is wrapped around the histone octamer. The results from these three studies have helped us to understand the role of core histone tail domains in the association of these complexes with nucleosomes and, broadly, the molecular basis of the transcription inhibitory potential of CHR in eukaryotes. We have employed spectroscopic techniques such as absorbance, fluorescence, and CD[1] to characterize the binding in detail. This has been followed by a biochemical approach such as gel electrophoresis to evaluate the nucleosomal DNA release potential of the complexes.

MATERIALS AND METHODS

Chromomycin, Tris, $MgCl_2$ solution (4.9 M), $CaCl_2$ (1 M), phenylmethanesulfonyl fluoride (PMSF), ethylenediaminetetraacetic acid disodium salt (EDTA), Triton X-100, micrococcal nuclease, trypsin immobilized on agarose beads, and calf thymus DNA were from Sigma Chemical Co. The buffer was prepared in quartz-distilled deionized water from a Milli-Q source (Millipore Corp.).

Preparation of the Nucleosome Core. Male albino Sprague-Dawley rats weighing about 150 ± 10 g, about 2−3 months old, were used throughout this work. Nuclei were isolated from the homogenized liver by the standard method (*21*), given briefly as follows. The liver was homogenized in 10 mM Tris-HCl buffer, pH 7.4, containing 0.3 M sucrose, 5 mM $MgCl_2$, 1 mM phenylmethanesulfonyl fluoride, 0.5% Triton X-100, and 40 mM sodium bisulfite. The homogenate was filtered through four layers of cheesecloth, followed by centrifugation at 800*g* for 10 min. The pellet was suspended in TM buffer (50 mM Tris-HCl buffer, pH 7.4, plus 10 mM $MgCl_2$) containing 2.2 M sucrose. The suspension was slightly homogenized and centrifuged for 1 h at 105000*g*. The pellet thus obtained was resuspended in TM buffer containing 1 M sucrose and centrifuged at 10000*g* for 10 min. The pellet obtained at this step contained nuclei. The outer membrane of the nuclei was removed by two successive washings with TM buffer containing 0.34 M sucrose and 1% Triton X-100.

Purified nuclei were digested with micrococcal nuclease to prepare the nucleosome core particle with a DNA length of 147 base pairs (*22*, *23*). One hundred microliters of the nuclear pellet (A_{260} = 228) was digested with 50 units of micrococcal nuclease for 5 min. The reaction was terminated with 30 mM EDTA. The digested nuclei were incubated in 10 mM $NaHSO_3$, pH 7.5, and 1 mM EDTA for 30 min and centrifuged at 10000*g* for 10 min. The supernatant contained mononucleosomes along with some longer chromatin fragments. At this stage the procedure described by Rao et al. (*23*) and Whittaker et al. (*31*) for selective solubilization of the mononucleosomes and of the core particles was used. NaH_2PO_4 [1.78% (w/v)] was added to the supernatant for the acidification of the mixture. The pellet obtained after centrifugation at 27000*g* for 10 min contained oligonucleosome, and the supernatant was enriched with the nucleosome core particles. The supernatant thus obtained was dialyzed against 0.01 M Tris-HCl, pH 7.5, containing 0.01 M EDTA and 0.002 M PMSF, and the dialyzed sample was finally concentrated. Final purification of the nucleosome core particle was achieved by centrifugation in 5%−20% (w/v) sucrose gradients. The purity of the nucleosome core particle was checked by identification of the histones in SDS−PAGE and acid urea gel after comparison with commercially obtained samples of histones (*24*). The purity of nucleosomal DNA was checked by agarose gel electrophoresis using a marker of 100 base pair DNA ladder. The concentration of nucleosome core particles was estimated in terms of DNA base. DNA was extracted from the nucleosome by repeated

[1] Abbreviations: F (au), fluorescence (arbitrary units); CD, circular dichroism; Tris, tris(hydroxymethyl)aminomethane.

phenol/chloroform extraction for quantitative estimation of base (*25*).

Preparation of the N-Terminal Chopped Nucleosome Core Particle. Nucleosome core particles were digested with trypsin immobilized on agarose beads for the removal of N-terminal tail domains from the core histones (*26*). Five hundred microliters of the nucleosome core particle (A_{260} = 200) in 10 mM Tris-HCl, pH 7.5, and 25 mM NaCl was digested with 28 units of immobilized trypsin for 45 min. SDS−PAGE of histone proteins before and after the chopping of N-terminal tail domains was done to check the proteolytic removal of N-terminal tails. N-Terminal chopped histones showed enhanced electrophoretic mobility in SDS−PAGE, which was in reasonable agreement with that reported in the literature (*26*).

Absorbance and Fluorescence Measurements. Absorption and fluorescence spectra were recorded with a Hitachi U-2000 spectrophotometer and a Shimadzu RF-540 spectrofluorometer, respectively. The absorption spectrum of CHR under different conditions was recorded in the wavelength range 520−360 nm. The concentration of CHR was estimated from a molar absorption coefficient of 8800 M^{-1} cm^{-1} at 400 nm (*6*). The fluorescence excitation wavelength was 470 nm instead of 400 nm in order to avoid photodegradation of the antibiotic (*6*). During fluorescence measurements, absorbance of the samples did not exceed 0.05 at 470 nm. Therefore, we did not correct the emission intensity for optical filtering effect.

CD Spectroscopic Study. CD spectra of both complexes in the presence of different polymers were recorded at room temperature in a cuvette of 1 cm path length using a Jasco J-720 spectropolarimeter. All spectra are the average of four runs. They were smoothed within the permissible limits by the in-built software of the instrument.

Analysis of Binding Data. Results from fluorometric titrations were analyzed by the following method. The apparent dissociation constant (K_d) was determined using a nonlinear curve fitting analysis (eqs 1 and 2). All experimental points for the binding isotherms were fitted by the least-squares method (*27*):

$$K_d = [C_0 - (\Delta F/\Delta F_{max})C_0][C_p - (\Delta F/\Delta F_{max})C_0]/[(\Delta F/\Delta F_{max})C_0] \quad (1)$$

$$C_0(\Delta F/\Delta F_{max})^2 - (C_0 + C_p + K_d)(\Delta F/\Delta F_{max}) + C_p = 0 \quad (2)$$

ΔF is the change in fluorescence emission intensity at 540 nm (λ_{ex} = 470 nm) for each point of titration curve, ΔF_{max} is the same parameter when the ligand is totally bound to polymer (N-terminal intact/chopped nucleosome core particle/naked DNA), C_p is the concentration of the polymer (N-terminal intact/chopped nucleosome core particle/naked DNA), and C_0 is the initial concentration of the antibiotic. A double reciprocal plot of $1/\Delta F$ against $1/(C_p - C_0)$ was used for determination of ΔF_{max}:

$$1/\Delta F = 1/\Delta F_{max} + K_d/[\Delta F_{max}(C_p - C_0)] \quad (3)$$

Details of the method and its origin are given in an earlier report from our laboratory (*5*). ΔF_{max} was calculated from the slope of the best fit line corresponding to the above plot. Since eq 3 is valid under the condition $C_p \gg C_0$, an 8-fold excess of the N-terminal intact/chopped nucleosome core particle/naked DNA was maintained during the collection of data for construction of the plot.

As described earlier (*7*, *10*), binding stoichiometry (expressed in terms of site size) was estimated from the intersection of the two straight lines of a least-squares fit plot of the normalized increase in fluorescence against the ratio of input concentrations of N-terminal intact/chopped core particle/naked DNA (in terms of DNA base) and the ligand(s).

Evaluation of Thermodynamic Parameters. Thermodynamic parameters, ΔH (van't Hoff enthalpy), ΔS (entropy), and ΔG (free energy), were determined using the equations (*28*):

$$\ln K_{app} = -\Delta H/RT + \Delta S/R \quad (4)$$

$$\Delta G = \Delta H - T\Delta S \quad (5)$$

R and T are the universal gas constant and absolute temperature, respectively. K_{app} (apparent equilibrium constant = $1/K_d$) was determined at three different temperatures, 10, 20, and 27 °C, respectively. The apparent equilibrium constant is the product of the intrinsic association constant and the stoichiometry of binding in terms of the number of ligands bound per nucleotide (i.e., reciprocal of the site size). ΔH and ΔS were determined from the slope and intercept of a plot of $\ln K_{app}$ against $1/T$. ΔG was determined from eq 5 after the incorporation of ΔH and ΔS values obtained from eq 4.

DNA Release Monitored by Agarose Gel Electrophoresis. Disruption of the N-terminal intact nucleosome core particle by complex I was checked as follows. Two hundred microliters of N-terminal intact nucleosome core particles (348 μM in terms of DNA base) in 10 mM Tris-HCl, pH 8.0, and 370 μM $MgCl_2$ was incubated with complex I (69 μM CHR plus 370 μM $MgCl_2$, in the same buffer) for 3 h at 30 °C. A small aliquot of this mixture was loaded into 1.5% agarose gel and run for 45 min. In the case of the N-terminal chopped core particle the experiment was repeated in the same way except the concentration of the N-terminal chopped nucleosome core particle was 225 μM in terms of DNA base and the concentration of complex was 45 μM in terms of CHR.

In the case of complex II, 200 μL of N-terminal intact core particles (630 μM in terms of DNA base) in 10 mM Tris-HCl, pH 8.0, and 4 mM $MgCl_2$ was incubated with complex II (126 μM CHR plus 4 mM $MgCl_2$, in the same buffer) at 30 °C for 3 h. A small aliquot of this mixture was loaded into 1.5% agarose gel and run for 45 min. For the disruption of the N-terminal chopped core, the experiment was repeated in the same way except the concentration of the N-terminal chopped core particle was 255 μM and the concentration of complex II was 51 μM in terms of CHR. In all cases control samples contain the same concentration of $MgCl_2$ as complex I or II with no antibiotic. A 147 base pair nucleosomal DNA was used as an internal marker to check the DNA release during the disruption process.

RESULTS

Changes in the absorption spectrum of complexes I and II upon binding to the N-terminal intact/chopped nucleosome

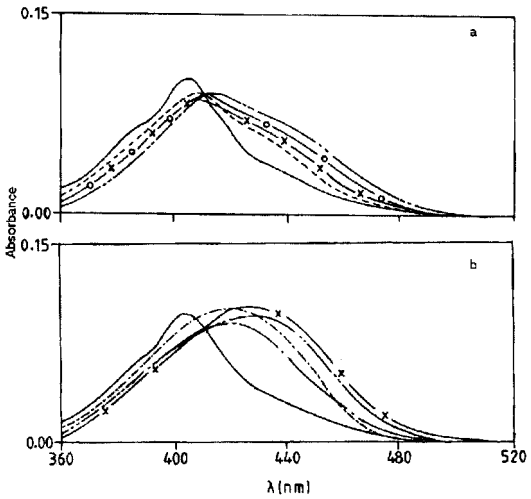

FIGURE 2: (a) Absorption spectra (360−520 nm) of CHR (11.2 μM, —) and complex I [CHR (11.2 μM) plus Mg^{2+} (300 μM)] in 10 mM Tris-HCl, pH 8.0 at 25 °C, under different conditions: alone (---) and in the presence of the N-terminal intact core particle (550 μM, — × —), N-terminal chopped core particle (350 μM, — ○ —), and naked DNA (350 μM, — -- —). (b) Absorption spectra (360−520 nm) of CHR (11.2 μM, —) and complex II [CHR (11.2 μM) plus Mg^{2+} (4 mM)] in 10 mM Tris-HCl, pH 8.0 at 25 °C, under different conditions: alone (---) and in the presence of the N-terminal intact core particle (750 μM, — - —), N-terminal chopped core particle (530 μM, — -- —), and naked DNA (400 μM, — × —).

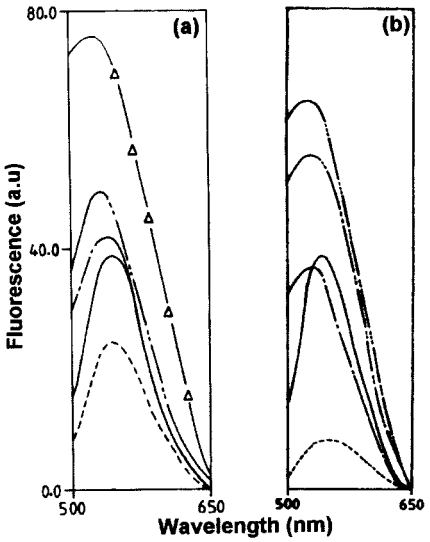

FIGURE 3: (a) Fluorescence spectra of CHR (8 μM, —) and complex I [CHR (8 μM) plus Mg^{2+} (300 μM)] in 10 mM Tris-HCl, pH 8.0 at 20 °C, under different conditions: in the absence (---) and presence of the N-terminal intact core particle (550 μM, — - —), N-terminal chopped core particle (350 μM, — -- —), and naked DNA (350 μM, — Δ —). (b) Fluorescence spectra of CHR (8 μM, —) and complex II [CHR (8 μM) plus Mg^{2+} (4 mM)] in 10 mM Tris-HCl, pH 8.0 at 20 °C, under different conditions: in the absence (---) and presence of the N-terminal intact core particle (750 μM, — - —), N-terminal chopped core particle (530 μM, — -- —), and naked DNA (400 μM, — --- —).

core particle and naked DNA originate from an association between them (Figure 2). The main features of the change are a red shift and broadening of the peak relative to that of the free antibiotic and complex I or II. There is a concomitant increase of the absorbance in the longer wavelength region. As reported earlier, these changes are characteristic of the association of the complexes with DNA (*5*, *6*). An interesting feature is that removal of N-terminal tail domains from core histones leads to a substantial alteration in the nature of the spectra when compared with the nucleosome core with the N-terminal intact.

Increase in fluorescence intensity of complexes I and II upon their association with the N-terminal intact/chopped core particle and naked DNA provided us the method to evaluate the binding parameters (Figures 3 and 4). In general, a blue shift of the emission peak accompanies the increase in fluorescence as a result of the association (Figure 3). The extent of the blue shift is comparatively more in the case of the N-terminal chopped core particle than the N-terminal intact core particle. Increases in the quantum yield and blue shift were earlier reported for the association of the complexes with free DNA (*6*). The related antibiotic mithramycin shows similar changes in fluorescence properties during its interaction with rat liver chromatin (*10*). Increase in fluorescence originates from a change in the local environment and/or conformation of the chromophore upon the formation of the complex with the N-terminal intact/chopped nucleosome core particle/naked DNA. Addition of the N-terminal chopped core particle leads to a greater enhancement in fluorescence quantum yield compared to the N-terminal intact core particle. The increase is more in the case of the bulkier complex II. The fluorescence quantum yield shows a further increase upon the depletion of total histone proteins from the nucleosomal DNA (Figure 3).

We estimated the binding parameters, binding constant, and stoichiometry for the ligand−polymer interaction from fluorescence titration of a particular ligand in the presence of varying concentrations of polymer. Representative titration curves for the interaction of complexes I and II with different polymers are shown in Figure 4. The nature of the curves indicates a noncooperative binding between complex I or II and polymers over the range of input concentrations of the polymer. Binding parameters were estimated from these isotherms as described under Materials and Methods. The inset to the figures illustrates how binding stoichiometry has been determined from the fluorescence titration data. Table 1 summarizes the binding parameters for the interaction of complexes I and II with different systems. The main points noted from the table are as follows. The presence of histone proteins in core particle reduces the binding affinity for both complexes, because both complexes bind to the naked DNA with comparatively higher affinity and lower stoichiometry in terms of DNA bases covered per ligand. Among the N-terminal intact and N-terminal chopped core particles, the binding affinity is lower in the case of the former. There is a 2-fold increase in the binding affinity after the tryptic removal of the N-terminal tail domains. From the N-terminal chopped to N-terminal intact core particles, there is also an increase in the binding stoichiometry in terms of covered base per drug molecule. The table shows that the effect of the N-terminal tail removal is more pronounced in the case of the bulkier complex II. Among the two types of complexes, I and II, the affinity constant and binding stoichiometry are in general different with the exception in the case of the N-terminal chopped core particle. However, the value of the dissociation constant at one temperature does not reflect the proper trend in the association with the core

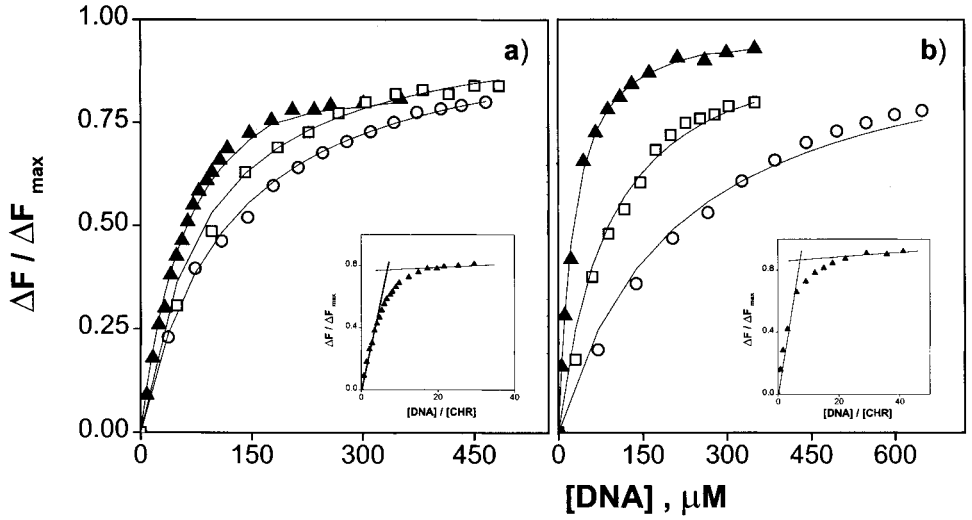

FIGURE 4: Curve fitting analyses to evaluate the dissociation constant for the association of complexes I (a) and II (b) with the N-terminal intact core particle (○), N-terminal chopped core particle (□), and dehistonized DNA (▲) in 10 mM Tris-HCl buffer, pH 8.0 at 20 °C. The fixed concentrations of complexes I and II used in titration with naked DNA were 8 and 13 μM, respectively. The inset in each panel illustrates the method to determine the binding stoichiometry associated with binding with the naked DNA (▲). The abscissa values corresponding to the intersection of the two straight lines for complexes I and II are 6.5 and 7.5, respectively, and give the value for the binding stoichiometry.

Table 1: Binding Parameters for the Interaction of CHR−Mg^{2+} Complexes with the N-Terminal Intact/Chopped Nucleosome Core Particle and Naked DNA in 10 mM Tris-HCl Buffer, pH 8.0 at 20 °C

ligand (CHR−Mg^{2+} complex)[a]	system	K_d[b] (μM)	n[c] (base/drug)
I	N-terminal intact core particle	116	18 ± 2
I	N-terminal chopped core particle	85	14 ± 1.5
I	naked DNA	54	6 ± 0.5
II	N-terminal intact core particle	210	31.8 ± 2.5
II	N-terminal chopped core particle	85	15.2 ± 0.5
II	naked DNA	20	7.4 ± 0.5

[a] The concentrations of Mg^{2+} used for the preparation of complexes I and II were 0.3 and 4.0 mM, respectively. [b] Apparent dissociation constants were obtained by the nonlinear curve fit method described under Materials and Methods. [c] Binding stoichiometry is expressed in terms of site size. It has been calculated from the titration profile using the method described in ref *7*.

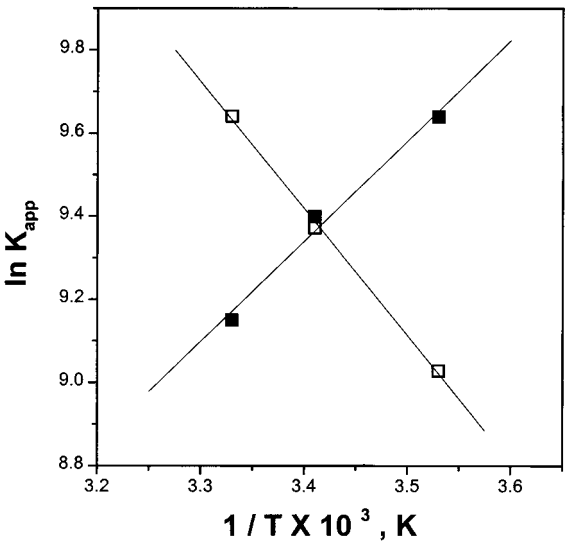

FIGURE 5: van't Hoff plots for the interaction of complexes I (■) and II (□) with the N-terminal chopped core particle in 10 mM Tris-HCl buffer, pH 8.0. The standard deviation of K_{app} values from three sets of experiments is 15%.

particle for the two types of complexes. Therefore, we evaluated the associated thermodynamic parameters.

Representative van't Hoff plots for the interaction of complexes I and II with the N-terminal chopped core particle are shown in Figure 5. Thermodynamic parameters for various systems estimated from such plots are summarized in Table 2. Association of complex I with different forms of the core particle is favored by enthalpy in contrast to the entropy-driven nature in the case of complex II. This trend is consistent with the earlier reports for calf thymus DNA (*5*, *6*).

After the removal of N-terminal tails from the nucleosome the contribution of negative enthalpy decreases for complex I; the negative contribution is compensated by a 4-fold increase in the entropy. The difference in the enthalpy contribution can be ascribed to the fact that N-terminal tails play a part in the noncovalent interaction with complex I. After the removal of N-terminal tails, complex I can access the minor groove better, as is evident from the greater degree of blue shift in the fluorescence peak of complex I during its interaction with the N-terminal chopped nucleosome. It leads to displacement of more water molecules from the minor groove. It will culminate in an increase of the value of the entropy change compared to the N-terminal intact nucleosome, because the displaced water molecules contribute to a positive change in entropy.

The case is radically different for the bulkier complex II; its binding is favored by entropy. There is a progressive increase in the positive enthalpy as we go over from the N-terminal core particle to naked DNA (Table 2). Simultaneously, there is an increase in the positive entropy. In naked DNA, minor groves of G/C-rich regions are relatively more accessible. The bulkier complex II is accommodated in the space of the minor groove via an increase in groove width accompanied by a B → A type transition in DNA conformation at the binding site (*7*). The above explanation for entropy increase is consistent with the proposition that the removal

Table 2: Thermodynamic Parameters for the Interaction of Complexes I and II with the Rat Liver N-Terminal Intact/Chopped Nucleosome Core Particle and Naked DNA in 10 mM Tris-HCl, pH 8.0 at 20 °C

system	ΔG (kcal/mol)	ΔH (kcal/mol)	ΔS (eu)
(a) complex I[a]			
N-terminal intact core particle	−5.3	−7.7	−8.1
N-terminal chopped core particle	−5.5	−4.8	2.2
naked DNA	−5.7	−5.2	1.7
(b) complex II[a]			
N-terminal intact core particle	−4.9	2.2	24.2
N-terminal chopped core particle	−5.5	6.0	39.2
naked DNA	−6.3	7.0	45.6

[a] The concentrations of Mg^{2+} used for the preparation of complexes I and II were 0.3 and 4.0 mM, respectively.

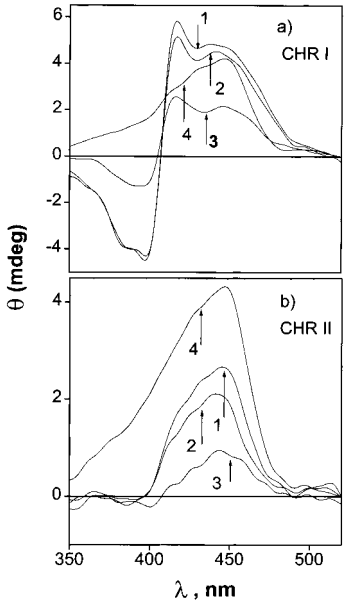

FIGURE 6: CD spectra (350−520 nm) of complexes I and II under different conditions in 10 mM Tris-HCl buffer, pH 8.0 at 25 °C: (a) complex I [CHR (15 μM) plus Mg^{2+} (300 μM)] (1), complex I in the presence of the 550 μM N-terminal intact core particle (2), complex I in the presence of the 350 μM N-terminal chopped core particle (3), and complex I in the presence of 350 μM dehistonized DNA (4); (b) complex II [CHR (15 μM) plus Mg^{2+} (4 mM)] (1), complex II in the presence of the 750 μM N-terminal intact core particle (2), complex II in the presence of the 530 μM N-terminal chopped core particle (3), and complex II in the presence of 400 μM dehistonized DNA (4). Note that the concentrations of polymer shown in the representative CD spectra above always correspond to the saturation concentrations.

of N-terminal tails enhances accessibility of the ligand to the minor grove of the G/C-rich region. This is consistent with the fluorescence spectra where association with naked DNA leads to maximum extent in blue shift of the fluorescence peak of complex II.

Figure 6 shows the CD spectra of complexes I and II, respectively, in the presence of saturating concentrations of different polymers. Changes in the profile and band intensity of visible CD spectra of complexes I and II occur as a result of association with DNA in the N-terminal intact and chopped nucleosome core particle. That is why spectra of both complexes have been recorded in the presence of naked DNA for comparison. In any particular set, CD spectra of the complex pass through a single point at different input concentrations of the polymer, thereby suggesting the formation of a single type of complex (figure not shown). CD spectra of both complexes of chromomycin are different in the presence of the N-terminal intact/chopped nucleosome core particle and naked DNA. The red shift of the peak in the CD spectra of both complexes upon addition of the N-terminal intact/chopped nucleosome/naked DNA is a common feature.

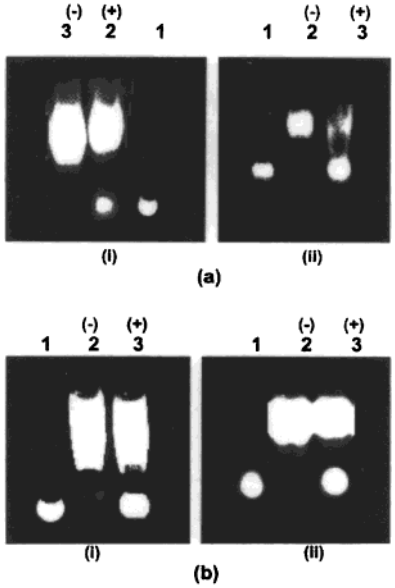

FIGURE 7: Agarose gel electrophoresis of the N-terminal intact core particle (i) and the N-terminal chopped core particle (ii) in the absence and presence of complex I (a) and complex II (b). Different lanes contain the following samples: 147 base pair DNA marker (lane 1); N-terminal intact/chopped core particle (lanes 2 and 3). (+) and (−) signs on the top of a lane imply the presence or absence of the drug−Mg^{2+} complex, respectively. Details of the experimental protocol are given under Materials and Methods.

The CD spectral profile of complex I in the presence of the N-terminal intact core particle is not much altered; however, there is a marked reduction in the intensity of both positive and negative bands with the loss of hump in the negative band of complex I in the presence of the N-terminal chopped core particle. In contrast, parental spectral features of complex I are lost in the presence of naked DNA. The difference in the asymmetric environment of the chromophore in the complexes with N-terminal intact and chopped core particles is indicated from the difference in CD spectra of bound complex I.

Differences in spectra upon addition of the N-terminal intact/chopped nucleosome core particle and naked DNA are also apparent in the case of complex II. Association of complex II with the N-terminal intact and chopped nucleosome core particle leads to a reduction in band intensity of the chromophore. This is in contrast to the naked DNA where the association results in an enhancement of the band intensity. The difference in CD spectra can be ascribed to either or both factors: the difference in the accessibility of the ligands to DNA and the presence of the aromatic chromophore of histones in the vicinity of the chromomycinone chromophore. The second possibility appears to be remote, because the reported spectra are in the visible region.

Figure 7 shows the agarose gel electrophoresis of the N-terminal intact/chopped core particle in the presence and absence of complex I or II. From the figure it is clear that

complex I or II can disrupt both the N-terminal intact and chopped core particles, leading to release of free DNA. The effect is more pronounced with the N-terminal chopped core particle in the case of complex I. A comparison of the relative intensity of the bands corresponding to nucleosomal DNA and released DNA (see lane 3 in Figure 7b) indicates that the disruption of the nucleosomal structure by complex II occurs to a greater degree in the case of the N-terminal chopped core particle. Among the two ligands, it appears that complex I is more efficient in disrupting the nucleosomal structure. These results support the proposition that N-terminal tail domains play a role in maintaining the stability of the histone−DNA complex in the nucleosome core particle. Release of free DNA has also been reported when groove binder DAPI interacts with the reconstituted nucleosome (*29*).

DISCUSSION

Since the first report of the association of the transcription inhibitor CHR with chromatin (*20*), there has been a radical progress in the knowledge about chromatin structure and its various levels of organization. It has also become apparent that transcription machinery involving RNA polymerase has to contend with the repressive chromatin structures before it finds the target DNA sequence. Nucleosomes play a key role in controlling the transcription machinery. Changes in nucleosome arrangement including disruption, unfolding, and short-range lateral mobility have been related to changes in gene activity. Therefore, we have concentrated our studies on the nucleosome core particle.

We have demonstrated an interaction of both complexes of chromomycin with the nucleosome core particle and the role of N-terminal tail domains of core histones in the binding process. The presence of associated histone proteins in the nucleosome core particle has a negative effect upon DNA-binding potential and stoichiometry of both complexes of chromomycin (Table 1). None of the two ligands bind to any histone. Independent experiments using the fluorescence property of the antibiotic have shown the absence of such interactions (not shown). Our results clearly demonstrate that the presence of core histones adversely affects the binding of the complexes with nucleosomal DNA. During transcription, sequences such as enhancers and promoters become "hypersensitive" to the digestion by micrococcal nuclease due to dissociation of histones from the nucleosomal DNA providing the naked DNA regions more accessible (*33*, *34*). The higher affinity of both complexes of chromomycin for dehistonized DNA is relevant from this prospective.

N-Terminal tail domains of core histones also play a significant role in the negative effect upon DNA-binding potential and stoichiometry of both complexes. We notice a consistent increase in binding affinity and reduction in site size upon removal of N-terminal tail domains in the nucleosome core particle (Table 1). The effect is more pronounced for the bulkier complex II. Comparison of the spectroscopic features in the presence of the core particle with or without N-terminal tail domains further brings out the effect of the N-terminal tail removal upon the association. The extent of the blue shift of the fluorescence peak is more in the complex with the N-terminal chopped core particle (Figure 4), indicating a comparatively more hydrophobic environment of the bound chromophore site in the N-terminal chopped system. Analysis of the CD spectral features of the bound complexes also suggests that the chirooptical environments of the chromophore are different in the N-terminal intact and chopped core particle. These nonoverlapping spectroscopic features may be ascribed to a change in binding site environment and geometry after the removal of N-terminal tails.

If spectroscopic and binding data propose that N-terminal tail domains influence the interaction of CHR with the eukaryotic genome, associated thermodynamic parameters reinforce this observation. Table 2 shows that depletion of N-terminal tail domains in the nucleosome core culminates in a trend of ΔH and ΔS values more akin to the naked DNA. Collectively, all results suggest that N-terminal tail domains inhibit the access of both complexes of CHR to the eukaryotic genome.

Agarose gel electrophoretic experiments have shown that both complexes have a tendency to disrupt the nucleosome structure. The disruption is dependent upon the concentration of chromomycin and follows a very slow kinetics with a half-life in the order of hours (results not shown). This type of disruption has been earlier reported for the minor grove binder DAPI (*29*) and intercalators such as daunomycin, adriamycin, and ethidium bromide (*30*). It means that binding of the transcription inhibitor CHR, leading to structural disassembly, and the resultant DNA release would lead to the loss of the chromosomal DNA as the template in the first step of the expression of a gene. Our data demonstrate that the N-terminal chopped nucleosome is more susceptible to disruption by an external groove binder, chromomycin, compared to the N-terminal intact nucleosome. The observation implies that N-terminal tail domains have an important role in maintaining the structural integrity of the nucleosome probably by preventing the access of the anticancer antibiotic chromomycin to the nucleosomal DNA. From the present results we propose that these tail domains not only regulate the eukaryotic transcription but also reduce the binding potential of xenobiotics such as anticancer drugs to the eukaryotic gnome. Removal of N-terminal tails enhances the access of the anticancer antibiotic CHR to the nucleosomal DNA. Although N-terminal tails are structureless entities of the nucleosome (*12*), it appears from our data that they have a part in maintaining the structural integrity of the nucleosome.

Differences in the binding potential, binding stoichiometry, and associated thermodynamics support our earlier proposition that complexes I and II are different molecular species with distinctive three-dimensional structures (*5*, *6*, *35*). The difference in the extent of nucleosomal disruption by the two ligands (Figure 7) conforms to the separate identity of the two complexes as DNA-binding ligands even at the level of recognition of nucleosome structure, where DNA is wrapped around the histone octamer. Since the in vivo concentration of Mg^{2+} is high (10 mM), chances of formation of complex II are greater. However, formation of complex I cannot be ruled out under certain special conditions; e.g., there are reported fluctuations in the Mg^{2+} concentrations in carcinogenic tissues (*32*).

ACKNOWLEDGMENT

We thank Professor J. K. Dattagupta, Head of the Crystallography and Molecular Biology Division of our Institute, for making the Jasco J-720 spectropolarimeter available. We also thank Ms. Sangita Majee for participation in the initial phase of the work and Ms. Sukanya Chakrabarty for fruitful discussion.

REFERENCES

1. Calabresi, P., and Chabner, B. A (1991) in *The Pharmacological Basis of Therapeutics* (Goodman and Gilmann, Eds.) pp 1209−1263, Macmillan Publishing Co., New York.
2. Rohr, J., Mendez, C., and Salas, J. A. (1999) *Bioorg. Chem. 27*, 41−54.
3. Goldberg, I. H., and Friedmann, P. A. (1971) *Annu. Rev. Biochem. 40*, 775−779.
4. Aich, P., and Dasgupta, D. (1990) *Chem. Biol. Interact. 83*, 23−33.
5. Aich, P., Sen, R., and Dasgupta, D. (1992) *Biochemistry 31*, 2988−2997.
6. Aich, P., and Dasgupta, D. (1995) *Biochemistry 34*, 1376−1385.
7. Majee, S., Sen, R., Guha, S., Bhattacharya, D., and Dasgupta. D. (1997) *Biochemistry 36*, 2291−2299.
8. Keniry, M. A., Banville, D. L., Simmonds, P. M., and Shafer, R. H. (1993) *J. Mol. Biol. 231*, 753−767.
9. Gao, X., and Patel, D. J. (1990) *Biochemistry 29*, 1033−1040.
10. Mir, M. A., and Dasgupta, D. (2001) *Biochem. Biophys. Res. Commun. 280*, 68−74.
11. Kornberg, R. D., and Lorch, V. (1999) *Cell 29*, 285−299.
12. Van Holde, K., Zlatanova, J., Arents, G., and Moudrianakis, E. (1995) in *Chromatin Structure and Gene Expression* (Elign, S. C. R., Ed.) pp 1−26, Oxford University Press, Oxford.
13. Luger, K., Mader, A. W., Richmond, R. K., Sargent, D. F., and Richmond, T. (1997) *Nature 389*, 251−260.
14. Workman, J. L., and Kingston, R. E. (1998) *Annu. Rev. Biochem. 67*, 545−575.
15. Lee, D. Y., Jaffery, J., Pruss, D., and Wolfee, A. P. (1993) *Cell 72*, 73−84.
16. Ausio, J., Dong, F., and Van Holde, K. (1989) *J. Mol. Biol. 206*, 451−463.
17. Lee, D. Y., Hayes, J. J., Pruss, D., and Wolfee, A. P. (1993) *Cell 72*, 73−84.
18. Juan, L. J., Utley, R. T., Adams, C. C., Vettese Dadey, M., and Workman, J. L. (1994) *EMBO J. 13*, 6031−6040.
19. Garcia-Ramirez, M., Dong, F., and Ausio, J. (1995) *J. Biol. Chem. 267*, 19587−19595.
20. Nayak, R., Sirsi, M., and Podder, S. K (1975) *Biochim. Biophys. Acta 378*, 195−208.
21. Blobel, G., and Potter, V. R. (1966) *Science 154*, 1662−1665.
22. Kornberg, R. D. (1900) *Methods Cell Biol. 170*, 1−25.
23. Rao, M. R. S., Rao, B. J., and Ganguly, J. (1982) *Biochem. J. 20*, 15−21.
24. Panyim, S., and Chalkley, R. (1969) *Arch. Biochem. Biophys. 130*, 337−346.
25. Burton, K. (1956) *Biochem. J. 62*, 315−323.
26. Ausio, J., Dong, F., and Van Holde, K. E. (1980) *J. Mol. Biol. 206*, 451−463.
27. Chakrabarty, S., Roy, P., and Dasgupta, D. (1998) *Biochem. Pharmacol. 56*, 1471−1479.
28. Castellan, G. W. (1989) *Physical Chemistry*, 3rd ed., p 799, Addision Wesley/Narosa Publishing House (Indian Student Edition), New Delhi, India.
29. Fritzgerald, D. J., and Anderson, J. N. (1999) *J. Biol. Chem. 274*, 27128−27138.
30. Grinmond, H. E., and Beerman, T. (1982) *Biochem. Pharmacol. 31*, 3379−3386.
31. Whittaker, R. G., Blanchard, B. J., and Ingram, V. M. (1979) *Anal. Biochem. 92*, 420−427.
32. Sigel, H., and Sigelds, A. (1990) *Metal Ions in Biological Systems* (Compendium on Magnesium and Its Role in Biology, Nutrition and Physiology) Vol. 26, pp 2−4, 243−247, Dekker, New York and Basel.
33. Wu, C. (1980) *Nature 286*, 854−860.
34. Almer, A., and Horz, W. (1986) *EMBO J. 5*, 2681−2687.
35. Chakrabarti, S., Mir, M. A., and Dasgupta, D. (2001) *Biopolymers (Biospectroscopy) 62*, 131−140.

BI010731R